Journal of the Chinese Institute of Engineers
Vol. 35, No. 2, March 2012, 211–218

Small-scale projection lap-joint welding of KOVAR alloy and SPCC steel

Yung-Chang Chen[a], Kuang-Hung Tseng[b]* and Hsiang-Cheng Wang[a]

[a]*Department of Vehicle Engineering, National Pingtung University of Science and Technology, Pingtung 91201, Taiwan, ROC;* [b]*Institute of Materials Engineering, National Pingtung University of Science and Technology, Pingtung 91201, Taiwan, ROC*

(*Received 14 May 2010; final version received 26 October 2010*)

The objective of this study was to investigate the effect of projection heights and operating conditions on projection collapse, nugget size, and joint strength of KOVAR alloy and steel plate cold-rolled commercial (SPCC) grade in small-scale projection welding of dissimilar metals. All welds were produced with a capacitor charging power supply. Three projection designs with different heights were used. Harris and Riley-type projection was embossed on the SPCC steel sheets. Nugget size was estimated using a peel test. Joint strength was evaluated using a tensile-shear test. The results indicated that a low-level projection has a positive effect, increasing the load-bearing capacity of projection. The nugget diameter and joint strength increase as the weld current and projection height increase. Increasing the electrode force will produce a small nugget. Nugget size is a good indicator of the strength of the welded joint. This study also found that a cold-collapse ratio of approximately 25% produces the highest tensile-shear strength of small-scale projection lap-joint welds.

Keywords: small-scale welding; projection collapse; lap-joint

1. Introduction

Resistance welding is a group of joining processes in which coalescence is produced by the heat obtained from resistance of workpieces to current in a circuit of which the workpiece is a part and by the application of pressure. Resistance welding was invented in 1877 by Elihu Thomson, and has been extensively used since then in the manufacturing industries for joining metal sheets (Hamedi and Pashazadeh 2008). Resistance welding methods include spot welding, seam welding, projection welding, flash welding, upset welding, percussion welding, and high-frequency resistance welding. Projection welding is primarily used to join a stamped or machined part to another part. One or more projections are produced on the parts during the forming or machining operations. The purpose of projection is to localize the heat and pressure at a specific location on the workpiece to be welded. Projection must be designed to support the electrode force to obtain a high contact resistance at the faying surface. Current flow through the faying surface between the two workpieces creates a rapid temperature increase. Electrode force then causes the collapse of the heated projections, and the workpieces can be fastened together. In spot welding, the differences in workpiece thickness and material properties generate unequal thermal load distributions that cause inconsistent weld quality (Zhou *et al*. 2000, 2001, Jou 2001, 2003, Xu *et al*. 2007). As a result, the projections are designed to create a uniform heat balance between workpieces with different thermal loads. Various carbon and alloy steels, and some coated steels can be projection welded. Harris and Riley (1961) reported that projection welding is an efficient practice for metal sheet fabrication and assembly.

In a capacitor charging power supply unit, the capacitor is charged *via* the controlled energy source and, the stored energy is first discharged through a high-performance thyristor, then through a step-down transformer and into the nugget (Salzer 2004). The special design of transformer induces a high-weld current on the secondary side of the transformer that is then directly conducted to the electrode. Capacitor charging power supply units produce an extremely short time cycle, and are consequently well suited for welding coated steels, as well as metal sheets with different thicknesses or properties. Many process conditions determine the quality of projection welds. Some of these conditions include projection geometry, electrode material, electrode force, weld current, time cycle, and power supply (Hess and Childs 1947, Nippes and Gerken 1952, Harris and Riley 1961, Adams *et al*. 1965, Cunninghan *et al*. 1966, Sun 2000, Luo and Chen 2004).

*Corresponding author. Email: tkh@mail.npust.edu.tw

ISSN 0253–3839 print/ISSN 2158–7299 online

http://dx.doi.org/10.1080/02533839.2012.638527
http://www.tandfonline.com

In recent years, small-scale resistance welding has been widely used in the fabrication and assembly of electronic and medical components, as described by Zhou *et al*. (2000, 2001). Note that the difference between 'small-scale' and 'large-scale' resistance welding depends not only on the workpiece scale, but also on the weld current and electrode force used. Small-scale resistance welding is associated with thin metal sheets (about 0.1–0.5 mm), generates a relatively smaller nugget size, and thus requires a lower weld current and electrode force. Previous studies have investigated both small-scale spot welding (Ely and Zhou 2001, Dong *et al*. 2002, Tan *et al*. 2002, 2004, Chang and Zhou 2003, Farson *et al*. 2003, Chen and Farson 2004, Fukumoto *et al*. 2007) and large-scale projection welding (Adams *et al*. 1965, Cunninghan and Begeman 1965, 1966, Cunninghan *et al*. 1966, Sun 2001, Luo and Chen 2004, Tusek *et al*. 2005, Zhu *et al*. 2006). However, there remains a lack of understanding of small-scale projection welding (SSPW) despite the increasing demand. Detailed experiments for this study were to investigate systematically the effect of projection heights and operating conditions on projection collapse, nugget size, and joint strength of KOVAR alloy to steel plate cold-rolled commercial (SPCC) steel dissimilar metal lap-joints. The application of the SSPW technique has also been demonstrated in this study.

2. Experimental procedure

The welded sheets used in this study included 0.25-mm thick ASTM F15 KOVAR alloy and 0.68-mm thick JIS G3141 SPCC steel. The lap-joints were made using sheets cut into strips (approximately 50 mm length and 10 mm width). Figure 1 shows a schematic illustration of the lap-joint geometry of welded sheets. Before welding, these strips were roughly polished with 400 grit SiC abrasive paper to remove the surface contaminants, and then cleaned using an ultrasonic bath containing an aqueous 30% acetone solution.

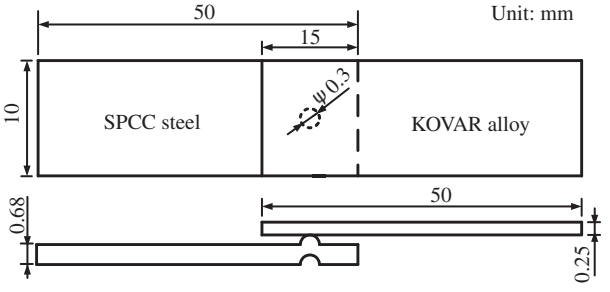

Figure 1. Schematic illustration of the lap-joint geometry of welded sheets.

The geometry and location of projection are critical in projection welding, which should be considered together with the material properties, especially when welding dissimilar metals. Heat balance in sheets with different thicknesses is maintained by placing the projection in the thicker of the sheets to be welded. Similarly, to maintain heat balance in metals with different properties, the projection should be placed on the metal with a higher thermal conductivity or lower electrical resistivity. As can be seen in Table 1 and Figure 1, the sheet thickness and thermal conductivity in SPCC steel is higher than that in KOVAR alloy. For this reason, the Harris and Riley-type projection was embossed on the SPCC steel sheets using punch and die sets. Three projection designs with different heights (0.10, 0.25, and 0.40 mm, respectively) were used in this study. Electrodes were straight cylinders of RWMA Class II type (chromium–copper) alloy with a 6-mm diameter flat-tip, and were not water cooled during the SSPW process.

All projection welds were produced with a capacitor charging power supply coupled to a pneumatically operated electrode. A capacitor charging power supply provided energy using a capacitor bank. The amount of energy delivered to the nugget was determined by the amplitude and duration of the current. The heat generation was controlled by varying the charge voltage on the capacitor bank. Experimental equipment had a rated heat input capacity of 3 kVA, while charge voltage levels varied from 25 to 450 V (DC). Table 2 presents the operating conditions including projection height, weld current, electrode force, squeeze time, weld time, and hold time.

Table 1. Physical properties of test specimens investigated.

Materials	Thermal conductivity ($W/m \cdot K$)	Electrical resistivity ($\mu\Omega \cdot cm$)
KOVAR alloy	17.5	294
SPCC steel	60.2	121

Table 2. Operating conditions for SSPW.

Projection heights	0.10, 0.25, and 0.40 mm
Weld currents	10.4–17.6 kA
Electrode forces	24.5–98.0 N
Squeeze time	83.3 ms
Weld time	16.7 ms
Hold times	16.7–166.7 ms

The nugget size was estimated by measuring the diameter of pullout buttons after the peel test. The joint strength was evaluated using a tensile-shear test that was performed using a HT-9102 computer servo control material testing machine.

3. Results and discussion

3.1. *Effect of electrode force and projection height on projection collapse*

The deformation collapse of projection is the key factor affecting the nugget size and joint strength. At the end of the squeeze cycle, cold-collapse of projection occurred and an area of intimate contact on the faying surface was established for the subsequent weld current to pass through. In this study, the amount of cold-collapse was measured using a three-dimensional surface profiler. The cold-collapse ratio (CR) can be calculated as

$$\mathrm{CR} = \frac{h_o - h_q}{h_o} \times 100\%, \tag{1}$$

where h_o is the height of the natural projection and h_q the height of the squeezed projection.

Sun (2001) reported that the amount of cold-collapse depends on the electrode force and projection geometry. Figure 2 shows the effect of electrode force and projection height on cold-collapse of projection after squeeze cycle. The height of the natural projection was maintained at a constant value, and revealed that the calculated CR value increases as the electrode force increases. The result clearly indicated that a high electrode force causes a large amount of projection collapse. It can also be seen in Figure 2 that the CR value for a 0.40-mm projection height increases from 6% to 45% as the electrode force increases from 24.5 to 98.0 N. Experimental results indicated a fairly steep slope at high-level projection. For the natural projection height of 0.10 mm, the slope of this curve is relatively flat. As the CR value increases from 9% to 22%, the electrode force again increases from 24.5 to 98.0 N. This may be because a low-level projection is more rigid than a high-level projection, and has a positive effect of increasing the load-bearing capacity of the projection structures. Figure 3 shows that a low-level projection is nearly uniform in cross-section throughout, however a high-level projection shows increasingly thinner neck-down region. A lower projection can enhance the neck-down region, resulting in a relatively small cold-collapse as the electrode force is applied.

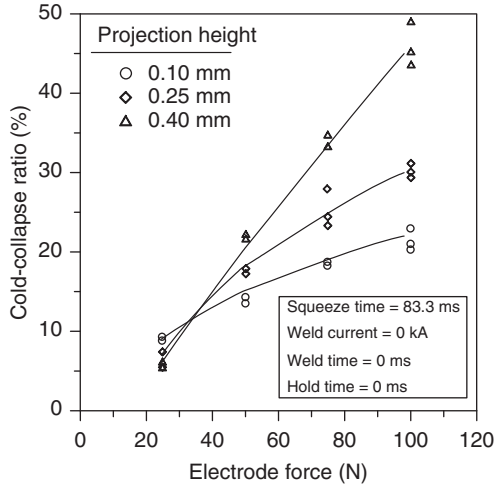

Figure 2. Effect of electrode force and projection height on CR.

3.2. *Effect of weld current and electrode force on nugget diameter*

The heat generation during resistance welding is given by the following expression (Joule heating principle):

$$H = I^2 Rt, \tag{2}$$

where H is the heat generation (J), I the weld current (A), R the resistance (Ω), and t the duration of current (s). The resistance includes contact resistance at the electrode/workpiece interfaces and at the faying surface between the two workpieces, and bulk resistance of base metals.

The weld current is the most important parameter in resistance welding, which determines the heat generated by a power of square, as shown in the Joule heating principle. As a result, the weld current is a main factor in determining the final nugget size (Sun 2000). Nugget size was determined by measuring the diameter of nugget observed on the fractured surfaces. Figure 4 shows the effect of weld current and electrode force on nugget diameter. As the weld current increases, the nugget diameter of the small-scale projection welds is increased. Due to the effect of

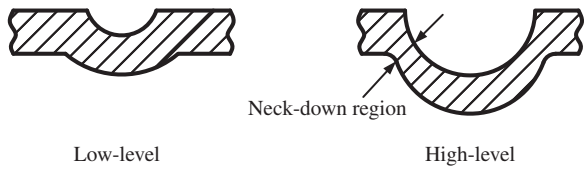

Figure 3. Comparison of low- and high-level projections.

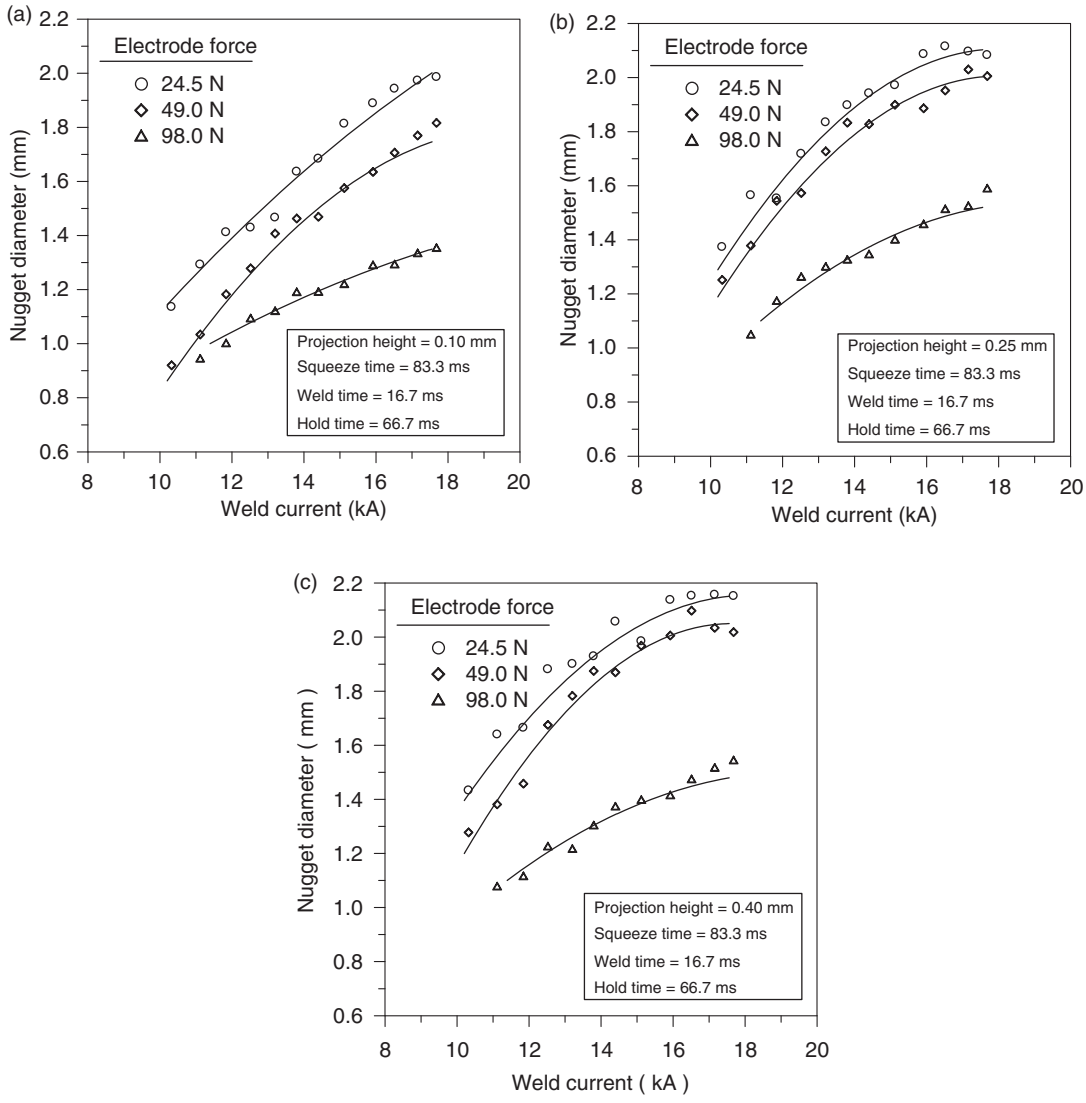

Figure 4. Effects of weld current and electrode force on nugget diameter; projection heights: (a) 0.10 mm, (b) 0.25 mm, and (c) 0.40 mm.

heat, as the weld current increases, the heat generation at the faying surface is increased. The nugget diameter is therefore also increased. In projection welding, the electrode force causes the projection collapse, which changes the contact area, and therefore the contact resistance. Increasing the electrode force will produce a larger contact area, resulting in a lower contact resistance at the faying surface. The contact resistance generally decreases with increasing temperature, and it almost proportionally decreases with the increasing pressure. As the electrode force increases, the contact pressure increases, thereby the contact area increases due to deformation of the faying surface asperities. As a result, the contact resistance at the faying surface decreases which reduces the heat generation and nugget diameter. Excessive electrode force will prematurely collapse the projection. It is therefore necessary to use a relatively high-weld current level to produce an acceptable nugget size. Experimental results indicated that the electrode force mainly affects the weld current thresholds for nugget initiation in projection welding. It should be noted that the electrode force must be low enough to give proper projection collapse without metal expulsion or electrode sticking, and yet high enough to produce a comparatively sound nugget.

Figure 4 also shows the effect of projection height on nugget size. The weld current and electrode force were maintained at a constant value, and it was found that the nugget diameter increases as the projection

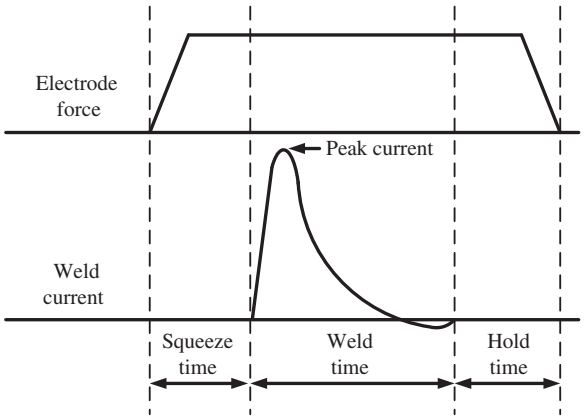

Figure 5. Time cycles for capacitor charging projection welding process.

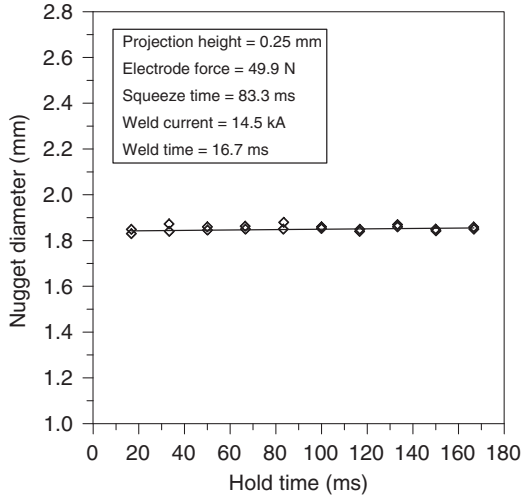

Figure 6. Effect of hold time on nugget diameter.

height increases. According to studies by Sun (2001), the faying surface contact area established due to the decreasing squeeze force with increasing projection height. Increasing the projection height will produce a smaller contact area at the faying surface, resulting in a high contact resistance. Since the calculated heat generation is directly proportional to the resistance, increased projection height has a positive effect of increasing the nugget diameter in projection welding.

3.3. *Effect of hold time on nugget diameter*

Figure 5 shows that the time cycles for capacitor charging projection welding basically consist of three periods: (1) squeeze cycle – the time that the electrodes contact the workpiece and establish the full electrode force before weld current is applied; (2) weld cycle – the time that the weld current is applied to the workpiece; (3) hold cycle – the time during which the electrode force is maintained to the workpiece after the last pulse of weld current ceases.

The projection height, electrode force, squeeze time, weld current, and weld time were fixed during projection welding experiments, while the hold time varied. Figure 6 presents the effect of hold time on nugget diameter. It can be seen that the final nugget diameter is not very sensitive to changes in hold time during SSPW. The average nugget diameter of small-scale projection welds increases from 1.8 to 1.9 mm, a change of about 5.6%, as the hold time increases from 16.7 to 166.7 ms. Weld current is turned off but electrode force is maintained during the hold cycle while the molten nugget is allowed to solidify. During the hold cycle of projection welding, the formation and growth of the molten nugget at the faying surface has been achieved, and therefore there can be no influence on nugget size. However, further study is needed to determine whether the resulting joint strength is acceptable or unacceptable. From a projection welding technical point of view, the hold time is necessary to allow the nugget to solidify before the electrode force is released, but it must not be too long as this may wear out the electrodes.

3.4. *Effect of weld current on joint strength*

Structures for resistance welds are usually designed, so that the joints are loaded in shear when the workpieces are exposed to tension or compression loading (Zuhailawati *et al*. 2010). In this study, the welded sheets were loaded in the tensile-shear direction in order to evaluate the strength of lap-joint welds. Figure 7 shows the effect of weld current on tensile-shear force. As the weld current increases, the tensile-shear force of lap-joint welds is increased. Based on the study of Adams *et al*. (1965), the joint strength is proportional to the nugget size. As a result, a slight increase in weld current rapidly increases the measured nugget diameter and, therefore, also the calculated tensile-shear force. Figure 7 also shows that the tensile-shear force of lap-joint welds increases as the projection height increases. Increasing the projection height will produce a larger nugget size, resulting in higher strength of the welded joint. In projection welding, a high strength of lap-joint welds is due to a large nugget size and not to the projection height in itself. This is because the projection height acts indirectly and actually the nugget diameter is the most significant factor affecting the joint strength.

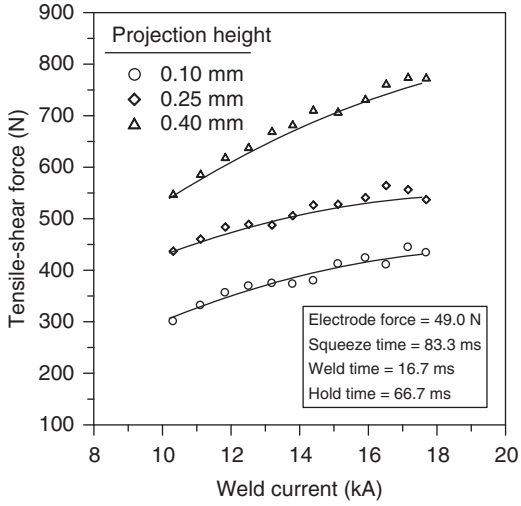

Figure 7. Effect of weld current on tensile-shear force of lap-joint welds.

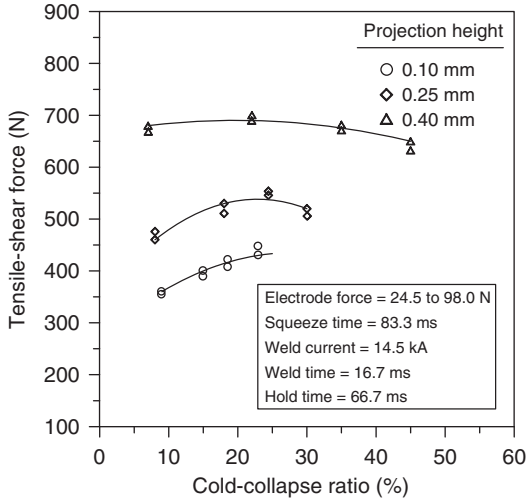

Figure 8. Effect of projection collapse on tensile-shear force of lap-joint welds.

3.5. *Effect of projection collapse on joint strength*

Figure 8 shows the effect of CR on tensile-shear force. It can be seen that a CR of approximately 25% produces the highest strength of small-scale projection lap-joint welds. The tensile-shear force increases to a critical point (CR equivalent to 25%), after which the strength of lap-joint welds decreases. Figure 9 shows the presence of the cavity within the nugget. This result suggests that the decrease in joint strength is mainly associated with the presence of the cavity. This is because the cavity reduces the effective load-bearing capacity in a unit area of nugget. The amount

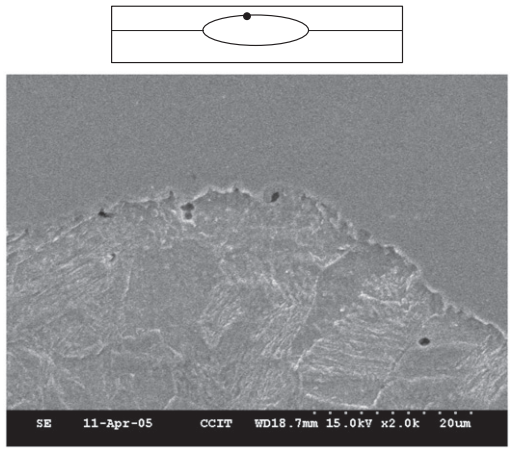

Figure 9. Scanning electron micrograph of a fracture surface (projection height 0.25 mm; weld current 14.5 kA; and electrode force 98.0 N).

of cold-collapse mainly depends on electrode force. During projection welding, the force applied to the electrode causes the collapse of projection and tends to change the nugget size. The electrode force should be adequate to flatten the projection completely before proper weld temperature is reached. However, excessive electrode force will prematurely deform the projection, and the nugget will have incomplete fusion or lack of fusion. Consequently, the joint strength will decrease. In addition, excessive electrode force levels also reduce the nugget size, and then the joint strength is also decreased.

3.6. *Technique application in transistor outline package*

Many industries currently use SSPW process to produce hermetic packages. Some uses include transistor outline packages, crystal oscillators, surface acoustic wave devices, medical implant devices, burst discs, relays, batteries, and pressure sensors (Salzer 2004). Transistor outline package is usually shaped like a can and is often called TO-Can. Figure 10 shows that a TO-Can usually consists of two main components: a cap is made of KOVAR alloy or some other metals which has appropriate mechanical and thermophysical properties, and a header is made of SPCC plated by nickel. Ring-type projection was designed in a header component. The header insures that the encapsulated components are provided with power, while the cap insures the smooth transmission of optical signals. Huang and Tseng (2009) reported that TO-Can can be successfully packaged using the proposed SSPW technique with a capacitor charging power supply.

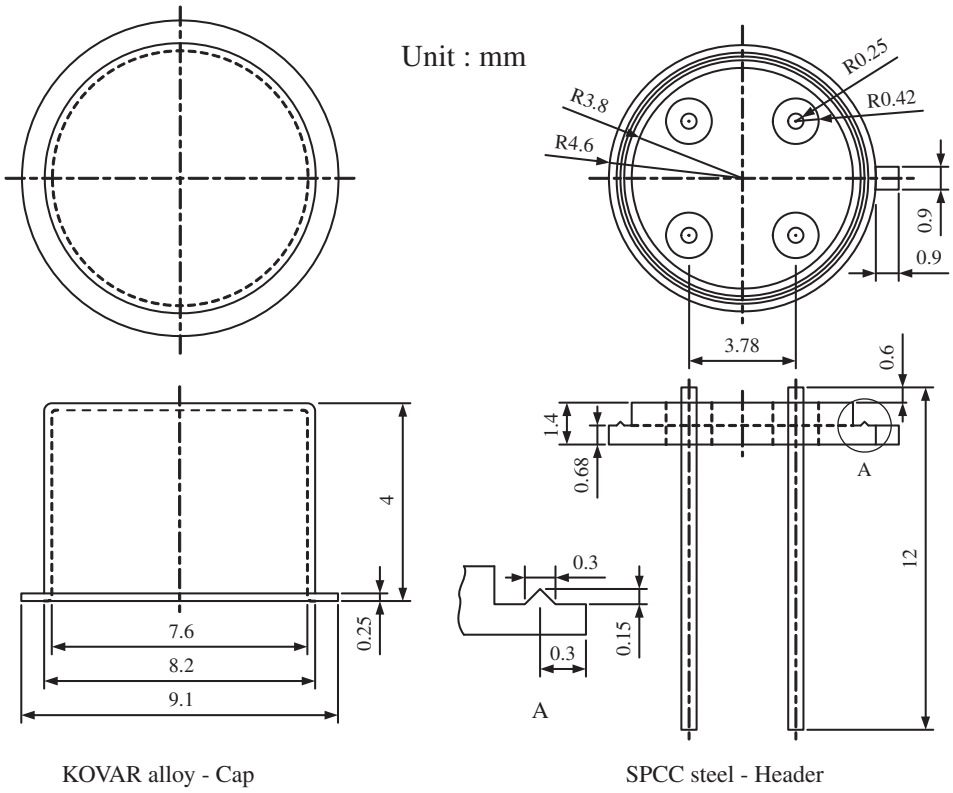

Figure 10. Package outline and typical dimensions for TO-Can.

4. Conclusions

This study conducted detailed experiments to investigate systematically the effect of projection heights and operating conditions on projection collapse, nugget size, and joint strength of KOVAR alloy to SPCC steel dissimilar metal in SSPW. All welds were produced with a capacitor charging power supply. The results can be summarized as follows:

(1) High-level electrode force and projection height cause a large amount of projection collapse. This is because a low-level projection is more rigid than a high-level one, and therefore has the positive effect of increasing the load-bearing capacity of projection.
(2) As the weld current and projection height increase, the nugget diameter of small-scale projection welds is increased. Increasing the electrode force will produce a lower contact resistance at the faying surface, resulting in a small nugget diameter.
(3) During the hold cycle of projection welding, the formation and growth of the molten nugget at the faying surface has been achieved, and therefore the hold time has no influence on nugget size.
(4) The tensile-shear force of lap-joint welds increases as the weld current and projection height increase. The nugget size is a good indicator of the strength of the welded joint.
(5) A cold-collapse of approximately 25% produces the highest tensile-shear strength of small-scale projection lap-joint welds.

Acknowledgments

The authors gratefully acknowledge the financial support for this research provided by the National Science Council, Taiwan, ROC, under Grant No. NSC 99-2221-E-020-006.

References

Adams, J.V., Matthews, G.N., and Begeman, M.L., 1965. Effect of projection geometry upon weld quality and strength. *Welding journal*, 44 (10), 466–470s.

Chang, B.H. and Zhou, Y., 2003. Numerical study on the effect of electrode force in small-scale resistance spot welding. *Journal of materials processing technology*, 139, 635–641.

Chen, J.Z. and Farson, D.F., 2004. Electrode displacement measurement dynamics in monitoring of small scale resistance spot welding. *Measurement science and technology*, 15 (12), 2419–2425.

Cunninghan, A. and Begeman, M.L., 1965. A fundamental study of projection welding using high speed photography. *Welding journal*, 44 (8), 381–384s.

Cunninghan, A. and Begeman, M.L., 1966. Effect of projection height upon weld quality and strength. *Welding journal*, 45 (1), 26–30s.

Cunninghan, A., Begeman, M.L., and Short, B.E., 1966. An analysis of the nugget formation in projection welding. *Welding journal*, 45 (7), 305–313s.

Dong, S.J., Kelkar, G.P., and Zhou, Y., 2002. Electrode sticking during micro-resistance welding of thin metal sheets. *Electronics packaging manufacturing*, 25 (4), 355–361.

Ely, K.J. and Zhou, Y., 2001. Microresistance spot welding of kovar, steel, and nickel. *Science and technology of welding and joining*, 6 (2), 63–72.

Farson, D.F., *et al*., 2003. Monitoring of expulsion in small scale resistance spot welding. *Science and technology of welding and joining*, 8 (6), 431–436.

Hamedi, M. and Pashazadeh, H., 2008. Numerical study of nugget formation in resistance spot welding. *International journal of mechanics*, 2 (1), 11–15.

Harris, J.F. and Riley, J.J., 1961. Projection welding low carbon steel using embossed projects. *Welding journal*, 40 (4), 363–376.

Hess, W.F. and Childs, W.J., 1947. A study of projection welding. *Welding journal*, 26 (12), 712–723s.

Huang, H.Y. and Tseng, K.H., 2009. Resistance projection welding for TO-Can style package. *Acta metallurgica sinica*, 22 (4), 255–262.

Jou, M., 2001. Experimental investigation of resistance joining for sheet metals used in automotive Industry. *Journal of Japan society of mechanical engineers C*, 44 (2), 544–552.

Jou, M., 2003. Real time monitoring weld quality of resistance spot welding for the fabrication of sheet metal assemblies. *Journal of materials processing technology*, 132, 102–113.

Luo, A.H. and Chen, G.L., 2004. Process analysis on a special projection welding with coupled FEM. *Materials science forum*, 471–472, 795–800.

Nippes, E.F. and Gerken, J.M., 1952. Projection welding of steel in heavy gages and in dissimilar thicknesses. *Welding journal*, 31 (3), 113–125s.

Salzer, T.E., 2004. Optimizing projection welding for hermetic sealing. *Welding journal*, 83 (3), 42–46.

Fukumoto, S., *et al*., 2007. Small-scale resistance spot welding of Zr based glassy alloys. *Materials science forum*, 561–565, 1307–1310.

Sun, X., 2000. Modeling of projection welding processes using coupled finite element analyses. *Welding journal*, 79 (9), 244–251s.

Sun, X., 2001. Effect of projection height on projection collapse and nugget formation - a finite element study. *Welding journal*, 80 (9), 211–216s.

Tan, W., Zhou, Y., and Kerr, H.W., 2002. Effects of Au plating on small-scale resistance spot welding of thin-sheet nickel. *Metallurgical and materials transactions A*, 33 (8), 2667–2676.

Tan, W., *et al*., 2004. A study of dynamic resistance during small scale resistance spot welding of thin Ni sheets. *Journal of physics D*, 37 (14), 1998–2008.

Tusek, J., *et al*., 2005. Direct resistance projection welding of copper and brass. *Science and technology of welding and joining*, 10 (1), 1–6.

Xu, J., *et al*., 2007. Optimization of resistance spot welding on the assembly of refractory alloy 50Mo-50Re thin sheet. *Journal of nuclear materials*, 366 (3), 417–425.

Zhou, Y., *et al*., 2000. Weldability of thin sheet metals during small-scale resistance spot welding using an alternating-current power supply. *Journal of electronic materials*, 29 (9), 1090–1099.

Zhou, Y., Dong, S.J., and Ely, K.J., 2001. Weldability of thin sheet metals by small-scale resistance spot welding using high-frequency inverter and capacitor-discharge power supplies. *Journal of electronic materials*, 30 (8), 1012–1020.

Zhu, W.F., *et al*., 2006. Numerical analysis of projection welding on auto-body sheet metal using a coupled finite element method. *The international journal of advanced manufacturing technology*, 28, 45–52.

Zuhailawati, H., *et al*., 2010. Spot resistance welding of a titanium/nickel joint with filler metal. *Welding journal*, 89 (5), 101–104s.